Evaluation of a new OGV architecture for an enhanced energy dissipation

Emmanuel Laroche, Philippe Reulet, David Donjat, Frédéric Deliancourt, Amélie Chassagne, Mohamed Boutaleb

Evaluation of a new OGV architecture for an enhanced energy dissipation

E. Laroche[(1)], P. Reulet[(1)], D. Donjat[(1)]

F. Deliancourt[(2)]

A. Chassagne[(3)], M. Boutaleb[(3)]

[(1)] ONERA/DMPE, Université de Toulouse, F31055 Toulouse-France, contact : emmanuel.laroche@onera.fr

[(2)]ONERA/DS, ONERA CS 70100, 73500 Modane

[(3)]Safran Aircraft Engines, Rond-Point René Ravaud, 77550 Moissy-Cramayel

Abstract

In the context of the ever increasing need to enhance engine cooling capability, a new heat exchanger/OGV architecture was defined and evaluated in CS2 framework. The design was validated based on wind tunnel tests carried out at ONERA Modane on two heated configurations. The numerical modelling of those tests confirms the expected thermal performance of the blade, with a very satisfactory agreement between numerical approaches and experimental results. Next steps include the optimization of the internal channel, in order to enhance the energy dissipation process.

Nomenclature

htc	Convective Heat Transfer Coefficient (W/m^2/K)
OGV	Outlet Guide Vane
OGV_HEX	Outlet Guide Heat Exchanger (oil) configuration
OGV_ELEC	Electrical Outlet Guide Vane configuration
M	Mach number at the inlet wind tunnel section
Mupogv	Mach number half a chord upstream of the OGV

1. Introduction/Context

The Non Propulsive Energy project in Cleansky 2 aims to analyze the potential of more electrical aircraft. To generate more electrical power, the implementation in the engine of electrical generators associated power electronics implies a high increase in thermal rejection that need to be evacuated with no size increase of the existing air/oil heat exchangers [1]. As a consequence, alternative solutions to increase cooling capability without impacting engine performance need to be analyzed.

One way considered by SAFRAN is to evacuate part of the energy through the fan Outlet Guide Vane (OGV). The OGV role can be seen as a heat exchanger allowing to evacuate part of the energy contained in the engine oil or/and electrical generators.

Preliminary studies were conducted at SAFRAN to define a heated OGV, where heat is brought via an oil exchanger and dissipated through the OGV metallic structure (Figure 1). This configuration, named OGV_HEX, was extensively examined by numerical modelling to derive low and high fidelity models. The high fidelity model corresponds to a fully conjugate simulation where the air around the blade, the blade itself, and the oil exchanger are meshed and simulated in a 3D model. The low fidelity model is based on a 1D modelling of the oil heat channel and a 3D thermal model for conduction inside the blade, with specified external heat transfer coefficient.

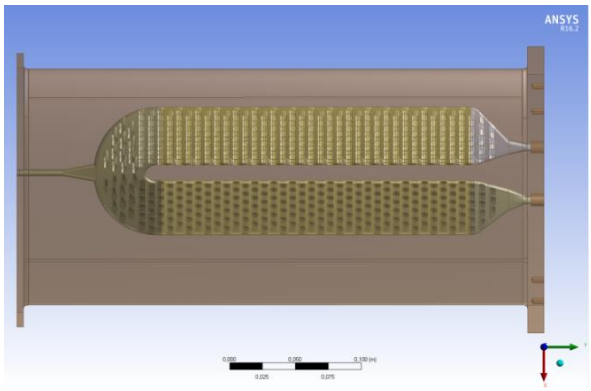

Figure 1 : OGV_HEX Reference Configuration

An experimental test campaign was planned to validate the concept and compare those numerical models with measured data. However, those measured data combine the influence of various parameters, such as the external and internal heat transfer coefficients. In other terms, identifying the origins of potential differences could be a difficult task, and one would like to be able to conduct a term by term verification. An uncertainty analysis not presented here shows that, on the internal walls of the blades, a prescribed heat flux condition (instead of an oil convective cooling) allows to minimize the uncertainty associated to the identification of the external heat transfer coefficient. That is why ONERA suggested an additional set-up (Figure 2), where the heat source is fully controlled through the use of electrical heaters.

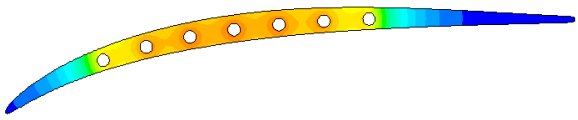

Figure 2 : Electrical OGV configuration : Blade Temperature field

In this alternative mock-up, the blade is heated through the use of seven electrical resistances. The number and location of heaters was determined to guarantee the smoothness of the temperature distribution, as well as its representativeness compared to the reference configuration. The following chapters describe the experimental mock-up developed, the measurements carried out on both configurations, and the associated validation.

2. Experimental mock-up

The tests were conducted in S3MA (ONERA Modane Avrieux) Wind Tunnel. The experimental mock-up can be visualized in Figure 3. A specific ceiling is part of the mock-up and the test section height is reduced compared to a classical configuration. The test section height corresponds to the OGV height, i.e. 375 mm. The S3MA Wind Tunnel inlet temperature is prescribed by the use of an accumulation heater upstream of the test section. The initial temperature is controlled by the heating power of this heater. The total temperature is not regulated and is monitored during the tests. Several pre-campaign tests were conducted to determine the best pre-heating strategy to guarantee an optimal temperature evolution during the tests. Contrary to the stagnation temperature, the stagnation pressure is regulated during the tests.

Figure 3 : Overview of the experimental mock-up integration in S3MA wind-tunnel

A schematic overview of the instrumented configuration can be visualized in Figure 4. Starting from the portside wall, only the second OGV is heated by an oil circulation or electrical power. The first and third OGV are instrumented with static pressures probes to estimate the isentropic Mach number distribution around the blade. The mock-up was designed to get a representative isentropic Mach number distribution for the heated OGV. The Mach number upstream of the vanes is estimated based

on eight static pressure probes located one half chord upstream of the vanes, and the total pressure probes present on the instrumented vanes. Concerning heat transfer measurements, the OGV_HEX and OGV_ELEC configurations are both instrumented with type K (Chromel/Alumel) thermocouples glued on the walls. Infrared Thermography measurements are conducted with a SC7750L (band III) camera on the optically accessible part of the suction side. The heated OGV as well as the instrumented ones are covered with a MAPAERO P10-X painting. The estimated thickness of the painting varies between 30 and 50 μm. Due to its possible influence on heat transfer, the average roughness Ra of the painting was measured between 0.5 and 1 μm. Such roughness levels are not expected to modify the measured heat transfer levels compared to a smooth configuration.

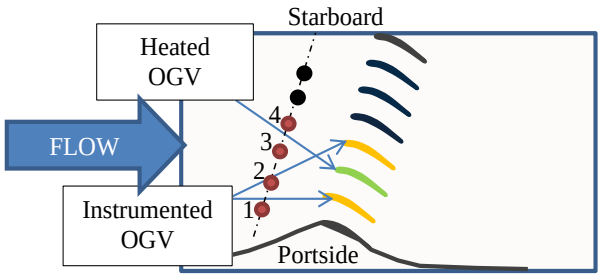

Figure 4 : Instrumented configuration overview

Concerning the oil loop, the flow rate is monitored during the tests, by a dedicated flowmeter. The temperature measurements in the oil channel (inlet and outlet) are performed through the use of PT100 probes. The heat flux dissipated through the heated OGV is estimated combining those data by a thermal balance.

As for the OGV_ELEC configuration, the resistance of each heater was measured at 20°C with a CALYS_150. The intensity being continuously monitored, this allowed to estimate the initial voltage, and therefore the global instantaneous power delivered to the 7 cartridge heaters, using the product of the (constant) voltage by the (instantaneous) intensity. The power delivered to each cartridge heater is then estimated based on its individual resistance compared to the total resistance of the heating system.

Considering the test campaign conducted, 23 points were covered varying

- the upstream OGV Mach number (from 0.21 to 0.59)
- the oil internal mass flow rate (from 100 to 900 l/h)
- the OGV type (ELEC/HEX)
- the oil channel matrix type (wavy or pin-fins)

For all tests, the stagnation pressure was prescribed at 1.5 bar, and the initial stagnation temperature was 25°C. Considering the heating of the OGV, several strategies were considered, from an initial ambient temperature to a warm-up before the wind gust.

3. Numerical simulation of OGV_ELEC configuration

For the OGV_ELEC configuration, a controlled heat flux distribution was prescribed on the internal wall of the blade. The obtained result at the blade surface was a temperature/heat flux distribution. The interest of developing a calculation methodology on the OGV_ELEC configuration was that the error obtained on the flux/htc distribution can be directly attributed to the methodology itself, and not to ill-controlled boundary conditions, which could be the case for the OGV_HEX configuration. From this, the convective heat transfer coefficient was calculated as:

$$h_{local} = \frac{q}{(T_{wall} - T_{adiab})} \quad (1)$$

The adiabatic temperature was assimilated to the recovery temperature (which is an intermediate between the static and the stagnation temperature). This recovery temperature was estimated through an isentropic Mach number:

$$T_{adiab} = rT_{t,0} + (1-r)\frac{T_{t,0}}{\left(1+\frac{\gamma-1}{2}Ma_{is}^{\ 2}\right)} \quad (2)$$

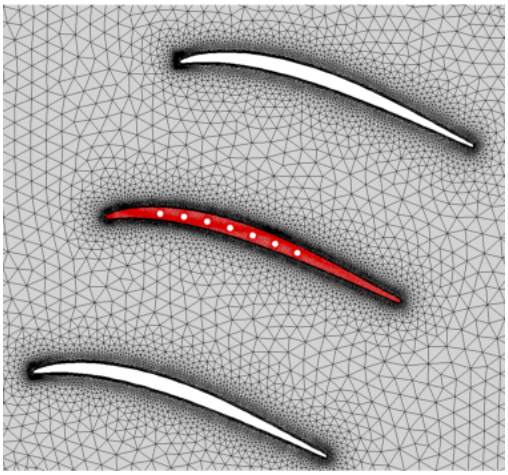

a)

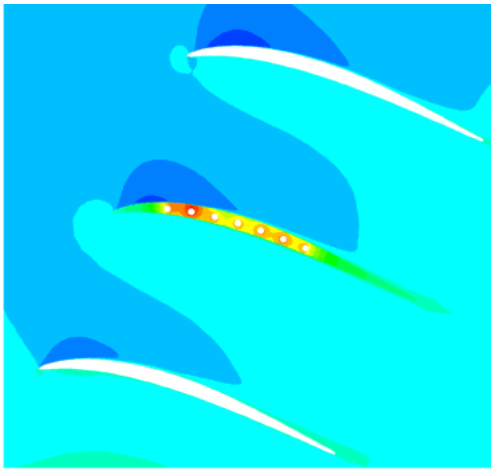

b)

Figure 5 : Mesh (a) and temperature map (b) for the conjugate simulation

where

$$Ma_{is} = \sqrt{\frac{2}{\gamma - 1}\left[\left(\frac{P_{t,0}}{P_s}\right)^{\frac{\gamma-1}{\gamma}} - 1\right]} \qquad (3)$$

with a recovery factor r=0.9.

Three test conditions were reproduced and listed in Table 1. They correspond to three OGV upstream Mach number (M_{upogv}) values, respectively of 0.21, 0.44, and 0.59. The calculations were carried out using ONERA's in house CEDRE® solver.

RUN	-	**470**	**475**	**481**
Mach upstream	-	0.379	0.299	0.150
Mach OGV	-	0.586	0.440	0.212
Pi upstream	*Pa*	150030	150010	150080
Ti upstream	*°C*	15.1	15.0	15.0
Total Power	*W*	2497	2472	2475
P1	*W/m 2*	87263	86396	86482
P2	*W/m 2*	88909	88026	88113
P3	*W/m 2*	80265	79468	79547
P4	*W/m 2*	86028	85173	85258
P5	*W/m 2*	88498	87619	87705
P6	*W/m 2*	85205	84358	84442
P7	*W/m 2*	77796	77023	77099

Table 1 : Numerical simulation conditions

This platform was developed for both research and industrial applications, in the field of energetics and propulsion. The software architecture follows a multi-domain, multi-solver approach and accepts any general unstructured grid. Each physical system is treated by a dedicated solver: gas phase, dispersed phase, thermal fields in solids and radiation. Here, only the Navier-Stokes and conduction solver are used. Details about the CEDRE platform can be found in [2].

Coming to turbulence modelling, two models were considered: Menter k-ω SST, and Dutoya-Bertier k-l Model. The first one is a standard model [3], the second one was used to evaluate the sensitivity of the solution to turbulence modelling. Boundary conditions used for CEDRE/CHARME are listed in Table 2 (Menter k-ω SST model) and Table 3 (k-l model).

The upstream conditions were the same for all runs. The upstream Mach number was prescribed by adjusting the downstream static pressure.

Run	470	475	481
Pi upstream (Pa)	150028	150028	150028
Ti upstream (K)	288.15	288.15	288.15
k upstream ($m^2.s^{-2}$)	1	1	1
w upstream (s^{-1})	2000	2000	2000
Ps downstream (Pa)	121000	135500	146450

Table 2 : Boundary conditions for k-w SST simulations

Run	470	475	481
Pi upstream (Pa)	150028	150028	150028
Ti upstream (K)	288.15	288.15	288.15
k upstream ($m^2.s^{-2}$)	1	1	1
l upstream (m)	0.001	0.001	0.001
Ps downstream (Pa)	122200	134000	146000

Table 3 : Boundary conditions for k-l simulations

Considering material properties for conductive heat transfer in the solid, standard values for steel are used: ρ=8030 kg/m^3, c=502.5 J.kg^{-1}.K^{-1}, λ=16.27 W.m^{-1}.K^{-1}.

Considering transition modelling, no transition modelling is used for those calculations. For the k-l model, however a natural transition process occurred at a location close to experimental transition position. For the k-ω SST model, the influence of transition modelling on blade temperature was shown to be of second order, and therefore corresponding calculations are not reported here. Results are summarized in Figure 6 to Figure 8. For each of the figures, the positive curvilinear abscissa (s) corresponds to the suction side, the negative s to the pressure side. The IR symbols (red squares) correspond to the Infrared measurements, only available up to 50% of the suction side.

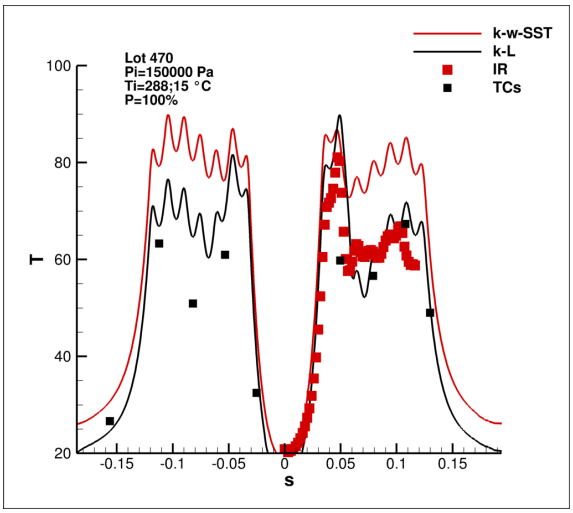

Figure 6 : Simulated/Experimental temperature profiles for run 470

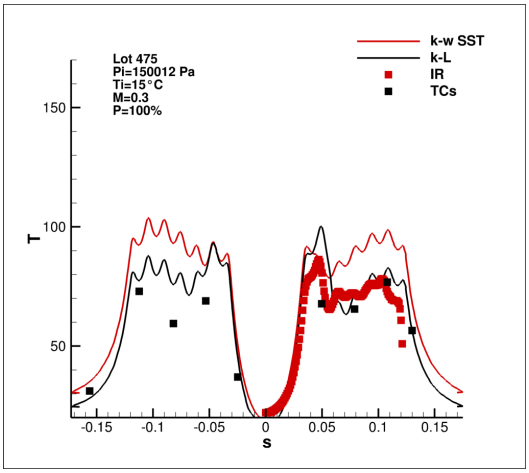

Figure 7 : Simulated/Experimental temperature profiles for run 475

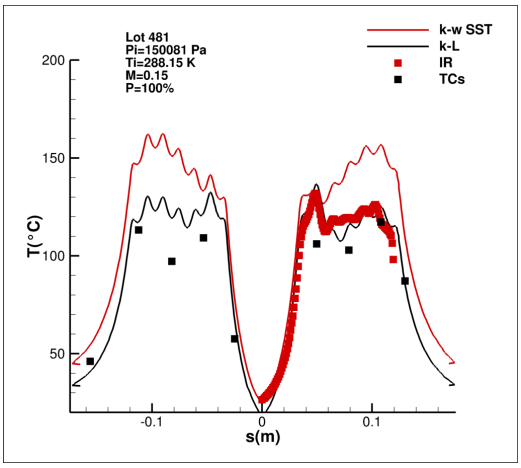

Figure 8 : Simulated/Experimental temperature profiles for run 481

The TCs (black squares) correspond to the thermocouples signals, available both on the suction side and the pressure side. The temperature levels provided by the thermocouples are generally lower than the ones estimated by the IR thermography. This is probably due to the glue used to set up the thermocouples. This glue creates an isolating layer and the thermocouple location can be visualized on the IR acquisitions as cold spots.

Figure 6 to Figure 8 exhibit the temperature distributions obtained for the three runs, with different freestream Mach numbers. The results obtained with Menter k-ω SST overestimate the measured temperature by around 20°C, whereas the k-l model simulations provide a satisfactory estimation, at least in the region where turbulence is established. The comparison is mostly done on the suction side, where IR measurements are provided, and can be compared with thermocouples data. Generally speaking the k-l model delivers on this configuration a lower blade temperature, which corresponds to a higher estimation of the heat transfer coefficient.

The htc distributions described in Figure 9 present the variation of the obtained htc with the upstream Mach number.

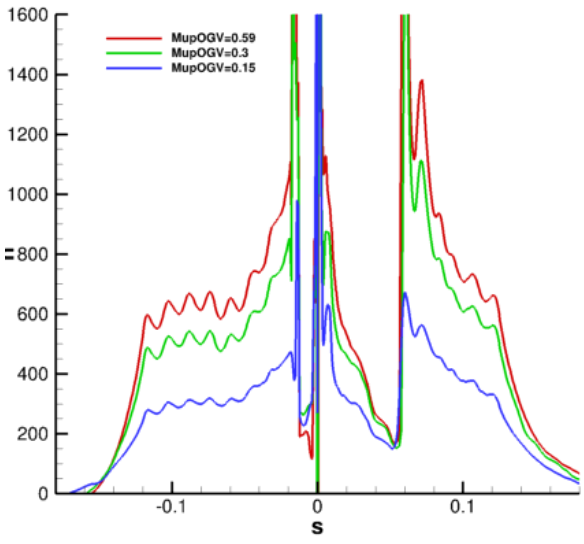

Figure 9 : Variation of htc with upstream Mach number (Mup OGV) for a conjugate model (k-l model)

This htc increases when the upstream Mach number increases. On the suction side, the first non-heated zone corresponds to a low heat transfer zone, except at the leading edge. This is also the case for the downstream area, after the heated zone. Taking into account conjugate heat transfers appears to be critical, in the sense that an isothermal calculation would conduct to a nearly constant htc for the downstream zone. The conjugate methodology (based on k-l model) presented here can therefore be considered as satisfactory to predict the blade temperature and the corresponding heat transfer coefficient. This methodology was therefore applied to the OGV_HEX case.

4. Numerical reproduction of Modane OGV_HEX tests

4.1. Methodology used

The external htc coefficient for the OGV_ELEC configuration was shown to be dependent on the temperature distribution on the blade. The OGV_ELEC should be seen as a well controlled set-up, used to validate a methodology which can be applied to the OGV_HEX (oil) configuration. In other terms, the methodology developed above has to be adapted to the OGV_HEX configuration to estimate the blade temperature. The fully consistent methodology would have consisted in running a fully conjugate simulation, with the oil channel, the blade and the wind tunnel air flow. However, this methodology was judged too costly and complex to apply. It was therefore suggested by ONERA to run a conjugate simulation of the oil channel and the blade, prescribing htc/reference temperature distributions at the blade outer surface. In this approach, the difficulty arising is specifying a realistic htc distribution at the blade surface. A first possibility would have consisted in specifying the distributions issued from the electrical OGV configurations. However, the temperature distributions in the two set-ups are fairly different, which will change the htc distribution. It was therefore suggested to run a first 3D conjugate simulation of the oil channel/blade configuration with uniform external htc condition to gain a first reasonable

temperature distribution. Then, a 2D simulation is run with the k-l model, to obtain a better estimate of the heat transfer coefficient. The objective of this 2D simulation is to estimate a htc distribution, with a representative wall temperature distribution, to minimize discrepancies aforementioned. The htc distribution is then modified, based on the OGV_ELEC temperature decrease in the downstream region to partially account for conductive effects (Figure 10). A conjugate simulation between the oil channel and the blade is then carried out. The (htc,Tref) distributions derived previously represent the external boundary condition of the blade model.

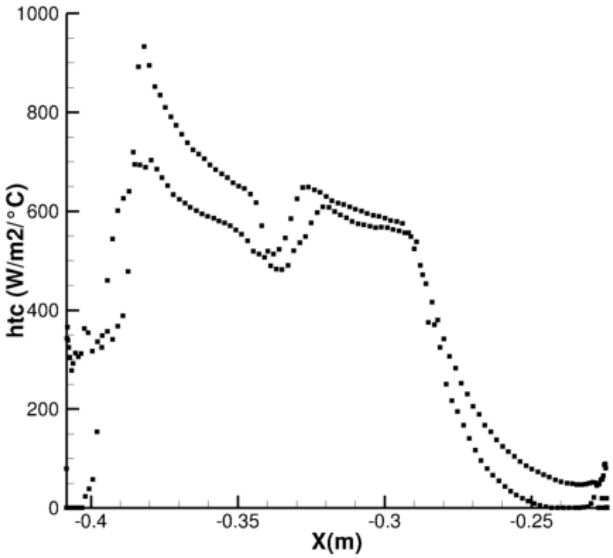

Figure 10 : HTC distribution (from 2D k-l simulation)

4.2. Conjugate model

The mesh was generated using CentaurSoft. One zone is dedicated to the oil channel, one zone to the blade. The geometry used was first provided from SAE (), and then a simplification/CAD cleaning process was achieved using Centaur. In particular, the blade hub and tip were suppressed to reduce the number of mesh elements required. The global number of elements generated is 43.7 M. tetraedra (36.1 M) are combined with prisms near the fluid wall (7.1 M) and pyramids (0.5 M) (will diminish gradually during the calculation due to the cooling process provided by the freestream.

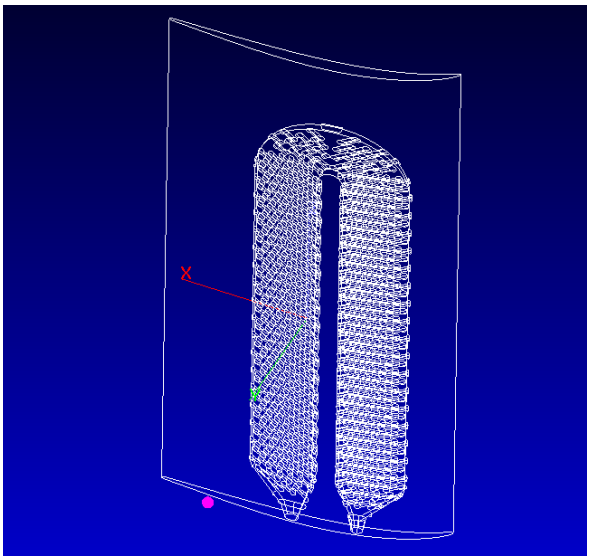

Figure 11 : OGV geometry used for meshing

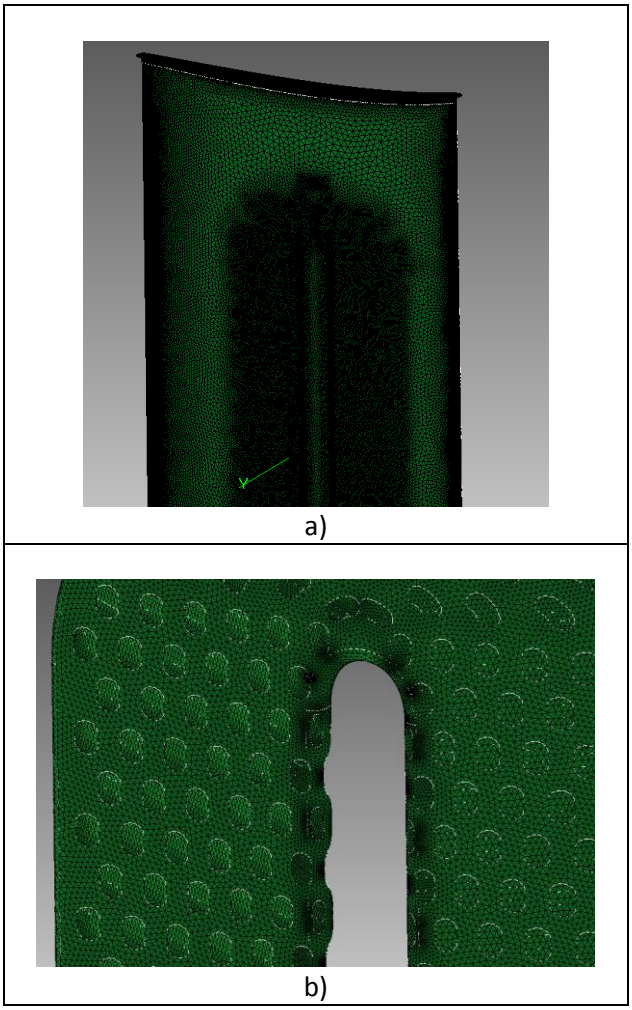

Figure 12 : Surfaces meshes for suction side (a) and internal matrix (b)

The initial solution for the fluid corresponds to the inlet values for oil temperature and outlet static pressure. The initial state for the solid is the oil inlet temperature. The temperature of the blade will diminish gradually during the calculation due to the cooling process provided by the freestream.

The inlet conditions for the freestream flow (Mach-mean, TI0), and the JET II oil flow (Qoil, TH_in) are listed in Table 4. For the cases studied, the freestream Mach number is constant and equal to 0.59. Only runs 3220, 3222 and 3221 were simulated, with an oil mass flow rate varying from 300 to 900 l/h. The oil inlet temperature also varies with the oil mass flow rate going from 155 to 160°C. In what follows, only run 3222 will be considered. However, similar trends were obtained for all runs.

Run	Mach_mean	Qoil_Lh	TH_IN	TI0_C
-	-	l/h	°C	°C
3221	0.59	300.6	155	15
3222	0.59	498.9	159	15
3220	0.59	898.7	160	15

Table 4 : Boundary conditions for the different OGV_HEX runs

IR measurements were post-processed as followed. The available data corresponds to a temperature mapping as plotted in Figure 13. 4 lines are then extracted corresponding to the vertical coordinates of available thermocouples and to 10 mm staggered lines (necessary for the IR analysis to avoid the lower temperatures due to the presence of thermocouples at the blade surface). Extracted temperatures profiles exhibit a transition process at x=40 mm, with a temperature decrease from x=40 to x=50 mm. The temperature appears to be minimal for x=85 mm, which corresponds to the material between the two passes of the oil channel.

Exact values at the thermocouple locations (+10 mm) are then extracted and compared to the CEDRE results. Here only suction side values are analyzed as the IR measurements are considered

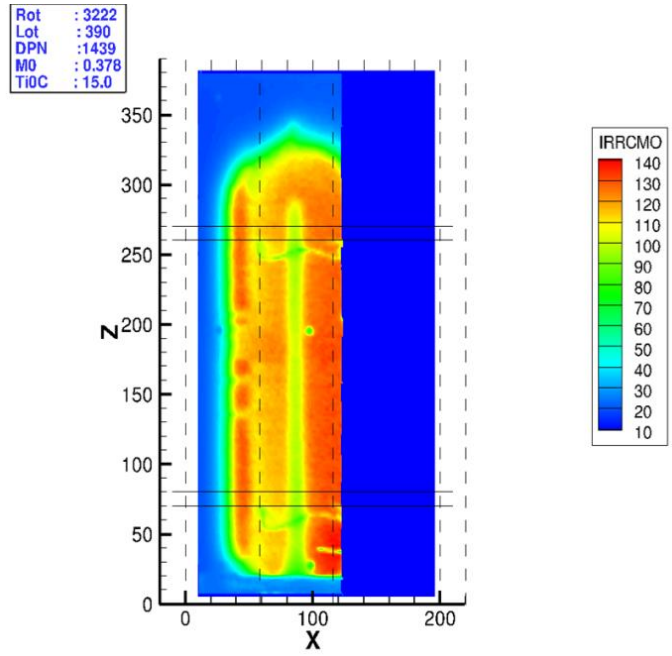

Figure 13 : IR map for run 390

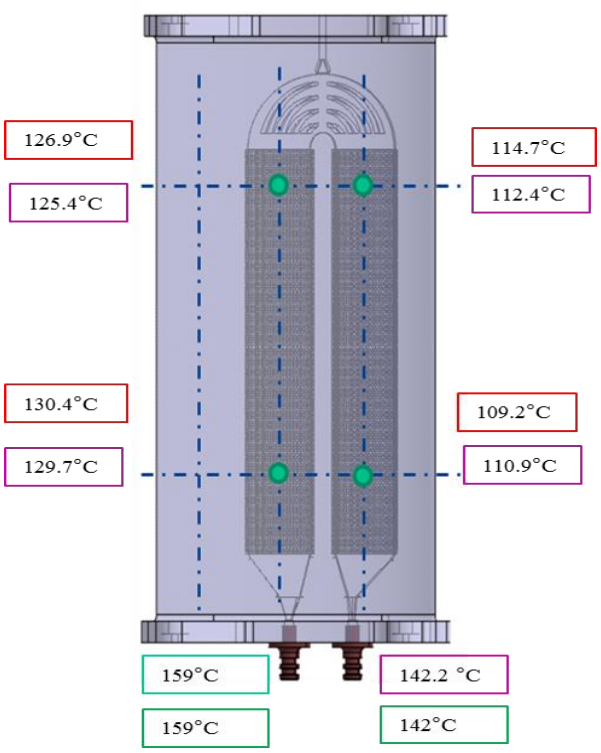

Figure 14 : Experimental/CEDRE temperature comparison (Run 3222)
(red IR, purple CEDRE, green PT100)

of better quality compared to thermocouple measurements.

Run 3222 is the performed simulation for the intermediate oil mass flow rate, around 500 l/h. The estimation of the temperature decrease through the channel appears to be very satisfactory, as the outlet temperature is estimated to be 142.2°C instead of a measured value of 142°C. Compared to the different IR measurements, CEDRE underestimates the temperature by less than 1 to 2.3°C, which appears to be under the measurement uncertainty of 4°C. This comparison validates the approach for blade temperature estimation, at least in the investigated area. More discrepancies are expected in specific areas such as the transition region, where the estimation of the htc is less accurate. The conclusions obtained for runs 3220 and 3221 are similar, with a very satisfactory agreement on wall temperature and dissipated power.

5. Conclusion

A new heat exchanger/OGV architecture was defined and evaluated in CS2 framework. A methodology was developed to assess the blade temperature distribution and the power dissipated in this OGV_HEX configuration.

An extra-mock up was specified and tested at ONERA MODANE to determine the external blade temperature, with well controlled boundary conditions. A conjugate simulation in close agreement with ONERA S3MA Wind-tunnel results then allowed to derive a realistic htc distribution for this OGV_ELEC configuration. Concerning the oil configuration, an initial estimation of the blade temperature was carried out at first. The htc distribution was then estimated for the OGV_HEX blade and used as an input for a 3D conjugate simulation of the oil channel/blade configuration. The blade temperature was then determined and a comparison with OGV_HEX experimental data available carried out. It was shown that the obtained results are very satisfactory, assessing oil temperature decrease through the blade for different oil mass flow rates, with less than 1°C discrepancy with measurements.

Future activities will focus on the improvement of the internal matrix, to optimize the internal htc. A dedicated generic experiment will be developed to validate the conclusion of this numerical study by measuring the temperature decrease obtained for different internal shapes.

References

[1] Lambert, P.A., Alejo, D., Fefermann, Y., Maury, C., Thoraval, B., Salanne, J.P., Isikveren; A.T., "Long-term hybrid-electric propulsion architecture options for transport aircraft"; Greener Aviation 2016; 1; Brussels; October 11-13; Paper 087

[2] Refloch, A., Courbet, B., Murrone, A., Villedieu, P., Laurent, C., Gilbank, P., Troyes, J., Tessé, L., Chaineray, G., Dargaud, J.B., Quémerais, E. & Vuillot, F., CEDRE software, Aerospace Lab J. n°2, 2011

[3] Menter, F. R., "Two-Equation Eddy-Viscosity Turbulence Models for Engineering Applications," AIAA Journal, vol. 32, no. 8, pp. 1598-1605, 1994

Acknowledgments

This project has received funding from the European Union's Horizon 2020 research and innovation program for the Clean Sky Joint Technology Initiative.